PHYSICAL REVIEW B **80**, 100301(R) (2009)

Evidence for hydrogen transport in deuterated $LiBH_4$ from low-temperature Raman-scattering measurements and first-principles calculations

R. Gremaud,[1,*] Z. Łodziana,[1] P. Hug,[2] B. Willenberg,[3] A.-M. Racu,[3] J. Schoenes,[3] A. J. Ramirez-Cuesta,[4] S. J. Clark,[5] K. Refson,[4] A. Züttel,[1] and A. Borgschulte[1]

[1]*Hydrogen & Energy, Empa, Swiss Federal Laboratories for Materials Testing and Research, Überlandstrasse 129, CH-8600 Dübendorf, Switzerland*

[2]*Solid State Chemistry, Empa, Swiss Federal Laboratories for Materials Testing and Research, Überlandstrasse 129, CH-8600 Dübendorf, Switzerland*

[3]*Institute of Condensed Matter Physics, Technische Universität Braunschweig, Mendelssohnstrasse 3, D-38106 Braunschweig, Germany*

[4]*ISIS Facility, Rutherford Appleton Laboratory, Chilton, Didcot, Oxon OX11 0QX, United Kingdom*

[5]*Department of Physics, University of Durham, Science Labs, South Road, Durham DHI 3LE, United Kingdom*

(Received 12 August 2009; published 10 September 2009)

We provide direct evidence for successive exchange of D atoms in the isotopically pure BH_4^- units of the crystalline solid lithium borohydride. We prove the coexistence of all $BH_{4-n}D_n^-$ $(0 \leq n \leq 4)$ units in the bulk by deconvolution of the D-stretching vibrations band of Raman spectra at 83 and 5 K in partially D-exchanged $LiBH_4$ and comparison with first-principles Raman intensity calculations. The measured distribution of $BH_{4-n}D_n^-$ units is in good agreement with a binomial distribution biased by H-D zero-point motions. This implies breaking the strong D_2 covalent bond and transport of hydrogen in $LiBH_4$ below the melting temperature.

DOI: 10.1103/PhysRevB.80.100301 PACS number(s): 66.30.jp, 63.20.dk, 78.30.Hv

Molecules can be weakly bound by dipole-dipole interactions such as in water or urea or contain significantly stronger bonds such as in KSCN (Ref. 1) or in complex hydrides.[2] Although the intermolecular forces between such molecules are weaker than the corresponding intramolecular ones, they are in many cases strong enough to form liquids or solids. Apart from its practical use for the structural description of such compounds, the concept of molecular entities within a solid helps for the understanding of many physical phenomena, in particular of electronic and chemical properties[3] and vibrations.[4]

In the complex hydride $LiBH_4$, the pseudomolecule BH_4^- is ionically bound to the counter ion Li^+. Phonons in $LiBH_4$ can be well approximated by so-called "internal" and "external" vibrations,[5] where "internal" refers to the characteristic vibrations of the BH_4^- ion, and "external" refers to the vibrational properties of the whole crystal structure. Accordingly, the labeling $\nu_{1,\ldots,4}$ of the internal vibrations is based on the vibrational modes of a free BH_4^- tetrahedral molecule, as the effect of the crystal field is small. While the concept of molecular units works well for hydrogen vibrations, it is debated whether it is appropriate for the description of hydrogen diffusion in complex hydrides. Within this concept, diffusion of hydrogen would require the diffusion of the whole pseudomolecule and/or its full disintegration.[6] However, the presence of H vacancies[7] or interstitial hydrogen[8] indicate that more probably diffusion of a fraction of the BH_4^- unit is the limiting factor for hydrogen transport in $LiBH_4$. Experimental issues make an understanding of the diffusion mechanisms even more difficult. In nuclear-magnetic-resonance (NMR) experiments, hydrogen and boron diffusion dominates molecular reorientations of the complex anion for temperatures above 440 K.[9] No H swapping between BH_4^- units could be observed by NMR on a time scale of ms below melting, suggesting that H transport in $LiBH_4$ is dominated by BH_4^- diffusion in the solid, such as in the liquid phase.[10] However, NMR cannot detect local H-diffusion processes, e.g., at the surface or at low-concentration defects. An alternative method to shed light onto the specific diffusion process is to label the diffusing atoms, experimentally realized by H-D exchange probed by Raman spectroscopy.[11]

In this Rapid Communication, we report on the effect of hydrogen-deuterium isotope exchange at 538 K on solid $LiBH_4$ with low-temperature Raman spectroscopy measurements. The experimental results are compared to density-functional theory (DFT) calculations of the vibrational spectra (frequencies and *intensities*) of $BH_{4-n}D_n^-$ species $(0 \leq n \leq 4)$, taken first isolated and then in the presence of the surrounding lattice. Our attention is focused on the 1550–1850 cm^{-1} B-D band, as it enables us to detect the presence of partially exchanged $BH_{4-n}D_n^-$ units and is not affected by strong Fermi resonances like the B-H band at 2200–2400 cm^{-1}. We furthermore determine the relative $BH_{4-n}D_n^-$ fraction as a function of the exchanged D-fraction x in $LiB(H_{1-x}D_x)_4$. This final static configuration gives crucial information on the hydrogen diffusion mechanism in this class of complex hydrides.

$LiBH_4$ is purchased from Sigma-Aldrich Fine Chemicals, Switzerland, (95%), and $LiBD_4$ from CatChem, Czech Republic (98%). H-D exchange in $LiBH_4$ is monitored by the mass change in a Rubotherm magnetic suspension balance. Three partially exchanged $LiB(H_{1-x}D_x)_4$ samples (300 mg) of nominal compositions $x=0.23$, 0.48, and 0.76 are obtained by exposing $LiBH_4$ to a 2×10^6 Pa D_2 gas pressure at 538 K for various time intervals (up to 23 h for $x=0.76$). The samples are handled solely in argon glove boxes for preparation and measured without contact to air. Raman spectra at 83 K are obtained with a Renishaw Ramascope 2000 of 1 cm^{-1} spectral resolution under 1 bar H_2 in a N_2-cooled Linkam THMS600 cell. The 633 nm line of the HeNe laser is focused on a 20 μm diameter spot, the laser beam power on

the sample being 2.8 mW. Raman spectra at 5K are recorded at the TU Braunschweig using a Jobin Yvon LabRam HR micro-Raman spectrometer of 2.3 cm^{-1} resolution adapted to a He cryostat. The 532 nm line of a diode-pumped Nd:YAG laser (50 mW output) is focused on an area of a few μm^2.

The normal-mode vibrational analysis of $LiBH_4$ and $LiBD_4$ was performed with *ab initio* lattice dynamics based on density-functional theory and the plane-wave pseudopotential method as implemented in the CASTEP code.[12,13] Pseudopotentials were of the optimized norm-conserving variety[14] with a plane-wave cutoff of 450 eV. Calculations were performed under the PBE approximation to exchange and correlation.[15] Brillouin-zone integration was performed according to the Monkhorst-Pack scheme with a $2\times3\times2$ mesh of k points, which gave convergence of all modes to a precision of better than 3 cm^{-1}. Pseudopotential errors in the frequencies were estimated at no more than 1% from a comparison of alternative pseudopotentials. The normal modes of the crystalline phase were determined from dynamical matrices calculated using density-functional perturbation theory (DFPT).[13,16] Raman tensors were calculated by numerical differentiation of polarizability tensors obtained using DFPT, and Raman intensities and activities were calculated using the formalism presented in ref. 17. Calculations for the isolated BH_4^- molecule were performed using the Gaussian program with the B3LYP functional and 6-311++$g(df,pd)$ basis set. For the mode analysis of partially exchanged $BH_{4-n}D_n^-$, hydrogen atoms were successively replaced by deuterium either in the BH_4 molecules or in the crystalline $LiBH_4$ unit cell. For the isolated molecule five configurations were considered, while for the crystalline phase we have considered exchange of the symmetry inequivalent H/D atoms, with all combinations for H-D exchange at 4c and 8d Wyckoff atomic positions.

Due to their large reduced mass difference, vibrational modes where mostly H atoms move (hereafter referred to as H vibrations) are easily distinguished in the $LiB(H_{1-x}D_x)_4$ Raman spectra from the modes where the amplitudes of D vibrations dominate (D vibrations). This technique is also very sensitive to gradual changes of the D fraction x. Furthermore, as the samples are transparent at the excitation and scattered wavelengths, the Raman spectra represent a bulk rather than a surface effect. Figure 1 presents Raman spectra for various partially exchanged $LiB(H_{1-x}D_x)_4$, from isotopically pure $LiBD_4$ to $LiBH_4$.

The internal vibrations are of particular interest for this letter, as they show the largest effects upon partial isotope exchange. These vibrations appear in the $LiBH_4$ spectrum as two well separated bands, corresponding to stretching, and, respectively, bending of the BH_4^- unit. Internal D vibrations in $LiBD_4$ show the expected isotope shift of about $\sqrt{2}$ with respect to H vibration.

For partially exchanged samples, the ratio between the integrated Raman intensity of the D-stretching region and the H+D-stretching regions is a good measure for the local deuterium fraction x in a particular grain.[18] The x values obtained from the Raman spectra are indicated in the figure. In the first place, the H-D exchange causes a transfer of intensity from the D- to the H-vibration modes. Additionally, for

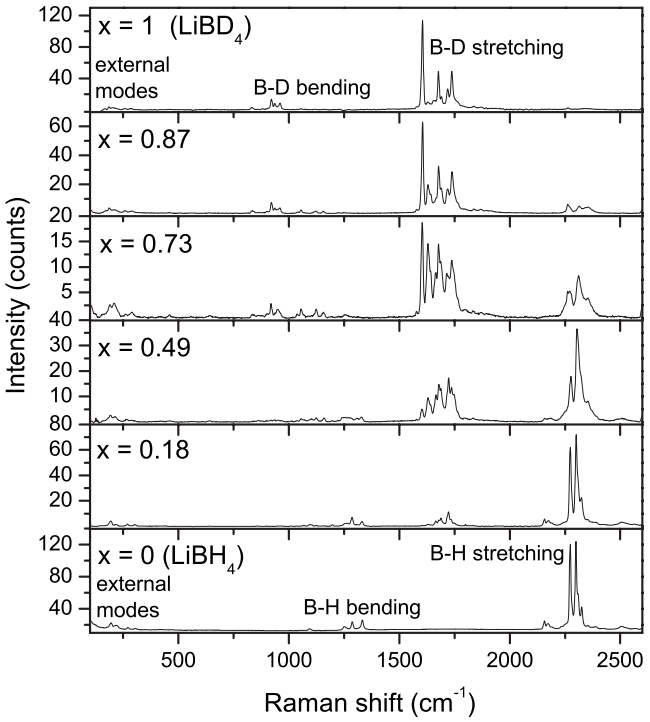

FIG. 1. $LiB(H_{1-x}D_x)_4$ Raman spectra at 83 K for various deuterium exchanged fractions x.

intermediate x values, new modes appear, which are not present in the isotopically pure compounds. These are most apparent in the center of the bending region and, most strikingly, within the D-stretching region.

The details of the D-stretching modes are shown in Fig. 2(a). For isotopically pure $LiBD_4$ (see upper panel), this region contains 4 doubly degenerate stretching modes labeled ν_1, ν_3, ν_3', and ν_3'' and 2 harmonics of the bending modes, $2\nu_4$

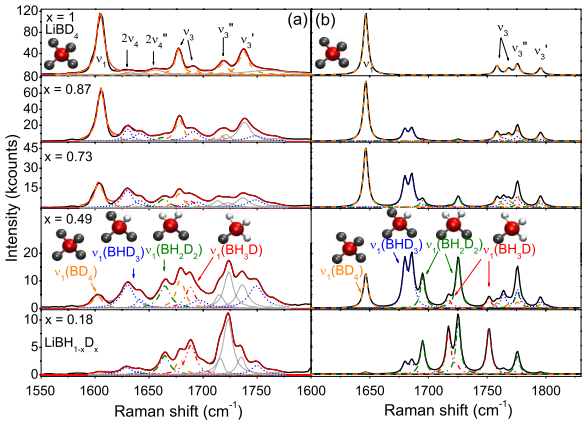

FIG. 2. (Color online) Boron-deuterium Raman stretching modes for various D-fractions x of $LiB(H_{1-x}D_x)_4$. (a) Measurement. The data are deconvoluted by fitting with lorentzian functions. (b) DFT calculation including Raman intensities. The intensity ratio between experiment and calculation is kept constant for all panels. Top panels: BD_4 vibrations (Ref. 19). All panels, *orange dashed line*: BD_4; *blue dotted line*: BHD_3; *green dash dotted line*: BH_2D_2; and *red dash dot dotted line*: BH_3D. *Full line* peaks arise from the contribution of several $BH_{4-n}D_n^-$ units.

TABLE I. Experimental symmetric stretching (ν_1) mode Raman frequencies [cm^{-1}] for the various $B(H_{4-n}D_n)^-$ units at 83 and 5 K compared to the theoretical values for the isolated cluster and periodic solid at DFT levels. Raman intensities are calculated with the CASTEP LR code and normalized to the intensity of the $\nu_1(BH_4^-)(A_g)$ mode. Modes with high (low) intensities are assigned $Ag(B_{2g})$ symmetry.

	Experiment (K)		Cluster Calc.		Crystal Calc.		D sites[a]
Unit	83	5	Frq.	Int.	Frq.	Int.	Wyckoff
BD_4^-	1605	1604	1606	0.71	1647	0.84	All
	–	1608			1646	$2\cdot10^{-5}$	All
BHD_3^-	1630	1620	1619	0.72	1680	0.70	$8d+4c_2$
	–	1627			1678	0.01	$8d+4c_2$
	1641	1633			1686	0.77	$8d+4c_1$
	–	1642			1687	0.01	$8d+4c_1$
$BH_2D_2^-$	–	–	1632	0.73	1695	0.44	$4c_1+4c_2$
	–	–			1702	$2\cdot10^{-3}$	$4c_1+4c_2$
	1664	1659			1725	0.72	$8d$
	–	1665			1731	$6\cdot10^{-4}$	$8d$
BH_3D^-	1688	1686	1645	0.74	1717	0.27	$4c_2$
	–	–			1724	0.03	$4c_2$
	–	1697			1751	0.25	$4c_1$
	–	–			1752	0.03	$4c_1$
BH_4^-	2298	2299	2270	1	2323	1	none
	–	2309			2323	$2\cdot10^{-3}$	none

[a]D positions after Ref. 23.

and $2\nu_4''$.[5,19] The ν_1 mode corresponds to four deuterium atoms vibrating in phase (symmetric stretching), while for the ν_3, ν_3', and ν_3'' modes, at least one deuterium atom vibrates in antiphase with respect to the others. Upon increasing H/D exchange, the intensity of the ν_1 mode strongly decreases, with no notable peak broadening or shift. This indicates that the number of BD_4 units decreases in the material, and the absence of shift confirms that the stretching modes are molecular vibrations, only weakly influenced by the surrounding lattice. Simultaneously, new modes, regularly spaced by approximately 30 cm^{-1}, appear between the preexisting ν_1 and ν_3 vibrations (1600–1700 cm^{-1}). We show in the following that these modes arise from the *symmetric* stretching of partially H-exchanged $BH_{4-n}D_n^-$ units, and label them $\nu_1(BH_{4-n}D_n)$, with $n=1,\ldots,4$ the number of D atoms in the unit.

The vibrational spectrum of isolated $BH_{4-n}D_n^-$ clusters predicts $\nu_1(BH_{4-n}D_n^-)$ modes spaced by about 13 cm^{-1} per H exchanged in BD_4^- (see Table I). This is a direct consequence of the Teller-Redlich rule,[20] which relates the frequency shifts in isotopically labeled molecules to the corresponding mass changes. It is remarkable that this rule holds also in first approximation for ionic solids such as $LiBH_4$. The absolute value of the frequency interval (13 instead of 30 cm^{-1} experimentally) is however underestimated in the cluster calculation, due to the proximity of the Li^+ cation in the solid. DFT calculations of the solid reproduce this interval and all the details of the experimental spectra: For the partially exchanged units (BHD_3^-, $BH_2D_2^-$ and BH_3D^-), the tetrahedral unit is slightly distorted in the solid and substitution at different crystallographic sites result in two different B-D bond lengths and Raman ν_1 frequencies. The crystal field splits further all modes,[19] making possible up to four modes per cluster type instead of one for the symmetric, isolated clusters. These four modes are resolved for the BHD_3 unit in the 5 K Raman spectrum of $LiB(H_{0.75}D_{0.25})_4$ in Fig. 3. In total, 9 out of the 14 symmetric D-stretching $\nu_1(BH_{4-n}D_n^-)$ vibrations are visible in this spectrum, evidencing the coexistence of *all* $BH_{4-n}D_n^-$ units in the same sample.

Moreover, the relative fraction of a particular H-D exchanged tetrahedral unit is directly given by its peaks area $\nu_1(BH_{4-n}D_n^-)$ normalized by the area of all ν_1 peaks. The experimentally obtained cluster distribution is compared in Fig. 4 with a Boltzmann statistical distribution $p(n,x)$ at the H-D exchange temperature, calculated from the zero-point vibrational energy difference E_n-E_m between $BH_{4-n}D_n^-$ units: $p(n,x)=\{\Sigma_{m=0}^{4}\exp[(E_n-E_m)/k_BT]\cdot f(m,x)/f(n,x)\}^{-1}$ with $f(n,x)$ the binomial distribution and k_B the Boltzmann constant. Both curves match well with each other, indicating that the five possible $BH_{4-n}D_n^-$ subunits are statistically dis-

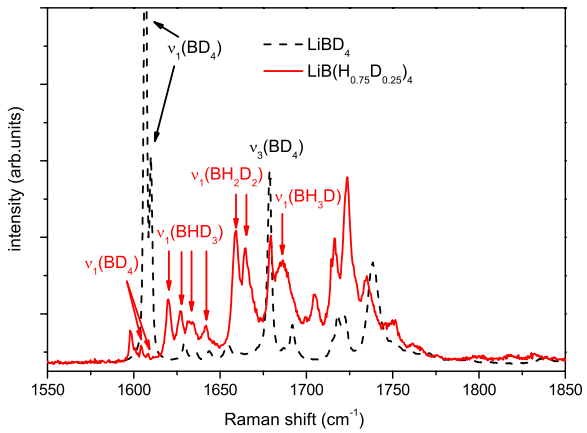

FIG. 3. (Color online) Raman B-D stretching modes for isotopically pure $LiBD_4$ (*black dashed line*) and $LiB(H_{0.75}D_{0.25})_4$ (*red full line*) at 5 K.

tributed in the compound. This makes possible the modeling of Raman spectra from the calculated DFT spectra and their direct comparison with the experimental spectra [Figs. 2(b) and 2(a)] The contribution in the calculated spectra of each $BH_{4-n}D_n^-$ unit is weighted by its fraction calculated from the statistical distribution at D-fraction x. The *ab initio* Raman spectra agree remarkably well with the measurements. In summary, low-temperature Raman measurements combined with DFT calculations of Raman intensity reveal complete scrambling of the hydrogen isotopes in the tetrahydroborates units. All $BH_{4-n}D_n^-$ units coexist in the bulk according to a Boltzmann distribution, demonstrating that even though the BH_4^- unit is very stable, hydrogen atoms are successively exchanged in the complex units. This confirms that the hydrogen atom is transported through the $LiBH_4$ crystal even at temperatures below melting. The exchange occurs most probably at low-concentration defects or at the surface, as the bulk-sensitive NMR technique could not evidence atomic H jumps.[9] Therefore, the net transport of atomic hydrogen in $LiBH_4$ most probably results from a combination of local H-exchange and subsequent mass transport. However, further research has to clarify whether the diffusing species is

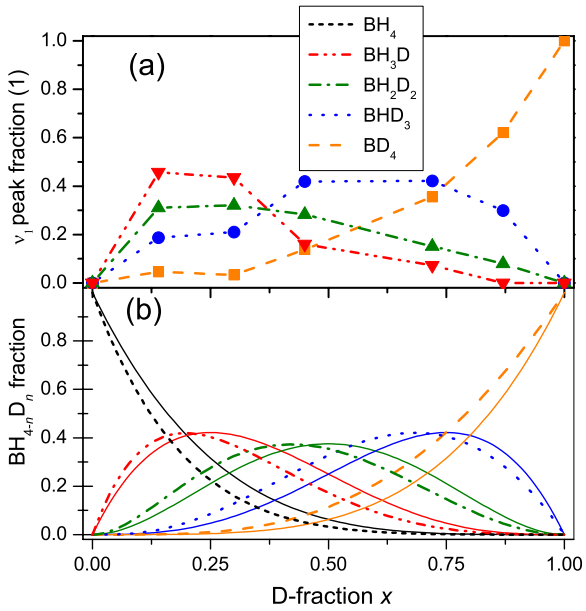

FIG. 4. (Color online) (a) Measured $BH_{4-n}D_n^-$ units distribution: relative $\nu_1(BH_{4-n}D_n^-)$ peaks area as a function of D-fraction x. (b) Calculated distributions: *Dash-dotted lines*, Boltzmann statistical distribution at 538 K from the zero-point vibrational energy difference between $BH_{4-n}D_n^-$ units. A binomial distribution (*thin full lines*) is shown for comparison.

H^+, H^-, H, H_2, and BH_3 or, e.g., BH_4^-.[9] An important implication of the statistical isotope distribution is that the strong covalent bond of the H_2 molecule is broken, either homolytically or heterolytically. These findings are compatible with a hydrogen transport facilitated by the presence of charged mobile point defects[21] (H^- and H^- vacancies[7] or BH_3 vacancies) similarly to $NaAlH_4$.[18,22]

This work was financially supported by the Swiss federal office for Energy via the CompHy project and by the European Commission, Contract No. MRTN-CT-2006-032474 (Hydrogen). Computing resources provided by the U.K. e-Science Centre, STFC (SCARF) and the Swiss Computer Center (CSCS, Manno) are gratefully acknowledged.

*robin.gremaud@empa.ch

[1] W. Schranz, Phase Transitions **51**, 1 (1994).
[2] P. Vajeeston *et al.*, Phys. Rev. B **68**, 212101 (2003).
[3] P. Vajeeston *et al.*, Phys. Rev. Lett. **89**, 175506 (2002).
[4] H. D. Lutz and H. Haeuseler, J. Mol. Struct. **511-512**, 69 (1999).
[5] K. B. Harvey and N. R. McQuaker, Can. J. Chem. **49**, 3282 (1971).
[6] A. J. Du, S. C. Smith, and G. Q. Lu, Phys. Rev. B **74**, 193405 (2006).
[7] S. Singh *et al.*, Acta Mater. **55**, 5549 (2007).
[8] R. Kadono *et al.*, Phys. Rev. Lett. **100**, 026401 (2008).
[9] R. L. Corey *et al.*, J. Phys. Chem. C **112**, 18706 (2008).
[10] D. T. Shane, R. C. Bowman, and M. S. Conradi, J. Phys. Chem. C **113**, 5039 (2009).
[11] A. Borgschulte *et al.*, J. Phys. Chem. A **112**, 4749 (2008).
[12] S. J. Clark *et al.*, Z. Kristallogr. **220**, 567 (2005).
[13] K. Refson, P. R. Tulip, and S. J. Clark, Phys. Rev. B **73**, 155114 (2006).
[14] M. H. Lee, Ph.D. thesis, Cambridge, 1995 (http://boson4.phys.tku.edu.tw/qc/my_thesis/index.htm).
[15] J. P. Perdew, K. Burke, and M. Ernzerhof, Phys. Rev. Lett. **77**, 3865 (1996).
[16] S. Baroni *et al.*, Rev. Mod. Phys. **73**, 515 (2001).
[17] D. Porezag and M. R. Pederson, Phys. Rev. B **54**, 7830 (1996).
[18] A. Borgschulte *et al.*, Phys. Chem. Chem. Phys. **10**, 4045 (2008). The relation between Raman intensities and D-fraction is derived from the present Raman DFPT calculation.
[19] A.-M. Racu *et al.*, J. Phys. Chem. A **112**, 9716 (2008).
[20] O. Redlich, Z. Phys. Chem. Abt. B **28**, 371 (1935).
[21] A. Peles and C. G. Van de Walle, Phys. Rev. B **76**, 214101 (2007); Z. Łodziana, A. Züttel, and P. Zielinski, J. Phys.: Condens. Matter **20**, 465210 (2008).
[22] Q. Shi *et al.*, J. Alloys Compd. **446-447**, 469 (2007).
[23] F. Buchter *et al.*, Phys. Rev. B **78**, 094302 (2008).